



Contents lists available at ScienceDirect

Spectrochimica Acta Part A: Molecular and Biomolecular Spectroscopy

journal homepage: www.elsevier.com/locate/saaA dual-channel colorimetric and ratiometric fluorescence chemosensor for detection of Hg²⁺ ion and its bioimaging applications

Palanisamy Ravichandiran^{a,g}, Vignesh Krishnamoorthi Kaliannagounder^{b,c}, Nikhil Maroli^d, Anna Boguszewska-Czubar^e, Maciej Maslyk^f, Ae Rhan Kim^g, Byung-Hyun Park^h, Myung-Kwan Hanⁱ, Cheol Sang Kim^{b,j}, Chan Hee Park^{b,j}, Dong Jin Yoo^{a,g,*}

^a R&D Education Center for Whole Life Cycle R&D of Fuel Cell Systems, Jeonbuk National University, Jeonju, Jeollabuk-do 54896, Republic of Korea

^b Department of Bionanotechnology and Bioconvergence Engineering, Graduate School, Jeonbuk National University, 567 Baekje-daero, Deokjin-gu, Jeonju-si, Jeollabuk-do 54896, Republic of Korea

^c Department of Bionanosystem Engineering, Graduate School, Jeonbuk National University, 567 Baekje-daero, Deokjin-gu, Jeonju-si, Jeollabuk-do 54896, Republic of Korea

^d Center for Condensed Matter Theory, Department of Physics, Indian Institute of Science, Bangalore 560012, India

^e Department of Medical Chemistry, Medical University of Lublin, ul. Chodźki 4A, 20-093 Lublin, Poland

^f Department of Molecular Biology, Faculty of Biotechnology and Environmental Sciences, The John Paul II Catholic University of Lublin, ul. Konstantynów 1i, 20-708 Lublin, Poland

^g Department of Life Science, Graduate School, Department of Energy Storage/Conversion Engineering, Hydrogen and Fuel Cell Research Center, Jeonbuk National University, Jeonju, Jeollabuk-do 54896, Republic of Korea

^h Department of Biochemistry, Jeonbuk National University Medical School, 567 Baekje-daero, Deokjin-gu, Jeonju-si, Jeollabuk-do 54896, Republic of Korea

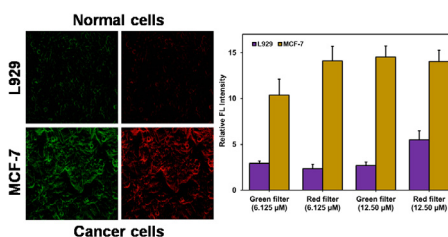
ⁱ Department of Microbiology, Jeonbuk National University Medical School, 567 Baekje-daero, Deokjin-gu, Jeonju-si, Jeollabuk-do 54896, Republic of Korea

^j Mechanical Design Engineering, Jeonbuk National University, 567 Baekje-daero, Deokjin-gu, Jeonju-si, Jeollabuk-do 54896, Republic of Korea

HIGHLIGHTS

- The chemosensor **4DBS** synthesized via greener and simple synthetic methods.
- The colorimetric and fluorescence recognition of Hg²⁺ ion was accomplished.
- The LOD for **4DBS** towards Hg²⁺ was 0.451 μM.
- Bioimaging of **4DBS** was accomplished in live cells and zebrafish larvae.
- **4DBS** showed the discriminative identification of Hg²⁺ in live cells.

GRAPHICAL ABSTRACT



ARTICLE INFO

Article history:

Received 13 January 2021

Received in revised form 28 March 2021

Accepted 30 March 2021

Available online 2 April 2021

Keywords:

Naphthoquinone probe

Metal ion fluorescence

Hg²⁺

Live cells

Cancer cells detection

Zebrafish imaging

ABSTRACT

A new colorimetric and ratiometric fluorescence chemosensor 4-((3-(octadecylthio)-1,4-dioxo-1,4-dihydrodronaphthalen-2-yl)amino)benzenesulfonamide (**4DBS**) was synthesized and investigated for the selective detection of Hg²⁺ in DMSO-H₂O (9:1, v/v) solution. The chemosensor was efficiently synthesized in two steps via Michael-like addition and nucleophilic substitution reactions. The ratiometric fluorescence turn-on response was obtained towards Hg²⁺, and its fluorescence emission peak was red-shifted by 140 nm with an associated color change from light maroon to pale yellow due to the intramolecular charge transfer effect. The formed coordination metal complex was further evaluated by FT-IR, ¹H NMR, and quantum chemical analyses to confirm the binding mechanism. The detection process was sensitive/reversible, and the calculated limit of detection for Hg²⁺ was 0.451 μM. Furthermore, **4DBS** was effectively utilized as a bioimaging agent for detection of Hg²⁺ in live cells and zebrafish larvae. Additionally, **4DBS** showed distinguishing detection of Hg²⁺ in cancer cells in comparison with normal

* Corresponding author at: R&D Education Center for Whole Life Cycle R&D of Fuel Cell Systems, Jeonbuk National University, Jeonju, Jeollabuk-do 54896, Republic of Korea.

E-mail addresses: ravichandru55@gmail.com (P. Ravichandiran), djyoo@jbnu.ac.kr (D.J. Yoo).

cells. Thus, **4DBS** could be employed as an efficient bioimaging probe for discriminative identification of human cancer cells.

© 2021 Elsevier B.V. All rights reserved.

1. Introduction

In humans or other life forms, metal ions play significant roles in biological processes such as metabolism, osmotic regulation, and cell signaling. Some alkali or alkaline earth metals such as copper, iron, zinc, and sodium ions at trace levels are beneficial to living systems [1,2]. Other heavy metals, including Hg^{2+} , Cd^{2+} , or Pd^{2+} ions, which are widely used in gold mining, coal plants, and mercury lamps, are widespread in water, soil, and air and can impart severe impacts to the environment and humans [3]. Among various heavy metals, mercury is well-known for its high toxicity even at a lower level, and due to the hazardous nature, its utilization is restricted in electronic appliances by the European Union's Restriction on Hazardous Substances (RoHS) [4]. The metal ion Hg^{2+} is easily propagated and can be introduced into the human body through respiration or absorption by skin and digestive tissues. After accumulation of Hg^{2+} ions at a certain level in the human body, high binding behavior with thiol groups in proteins and enzymes induces potential impairment of the kidneys, heart, brain, immune system, lungs, central nervous system and other tissues [5–8]. According to the U.S. Environmental Protection Agency (USEPA), the permissible level of Hg^{2+} contamination in drinking water is $2 \mu\text{g L}^{-1}$, and a maximum concentration of $5 \mu\text{g L}^{-1}$ leads to harmful effects in culture medium [9,10]. Thus, effective methods should be developed for monitoring and selective determination of Hg^{2+} ions in environmental and biological samples, which are of the highest requirement in the current circumstances.

Considering heavy metal pollution, over the past few decades, several efficient techniques have been examined in an overall large research effort. Of late, modern analytical techniques have often been employed for the quantitative and qualitative determination of heavy metals. These techniques include atomic absorption/emission spectrometry, capillary electrophoresis, high-performance liquid chromatography, gas chromatography, mass spectrometry, and electrochemical methods [11–16]. These analytical techniques are comprised of several practical advantages such as precise accuracy, high reliability, repeatability, and easy separation of selective analytes [17,18]. However, these analytical techniques also have several practical drawbacks including the need for complex instrumental operation, prolonged analysis time, utilization of expensive materials, sample preparations under hazardous conditions, and expensive instruments that require sophisticated maintenance [19]. Therefore, simple and efficient analytical techniques must be developed which allow rapid analysis, high selectivity, easy operation, and economic feasibility. Among various recent methods available for metal ion detection, optical chemosensor have attracted wide attention among researchers. In contrast, colorimetric and fluorescence chemosensor are known to be practically more advantageous, exhibiting real-time analysis, operational simplicity, highly reversibility, low detection limit, qualitative/quantitative detection of specific analytes while avoiding the utilization of complex analytical or spectroscopic techniques [20,21]. Over the past several years, varieties of colorimetric chemosensor have been developed that provide low-cost direct identification of analytes based on color. If the sensing output is a color change, this phenomenon can be easily recognized by the naked-eye or inexpensive instruments by a non-technical observer [22,23]. On the contrary, to overcome the practical disadvantages of modern analytical techniques, the

ratiometric approach is one of the efficient methodologies with good reliability for analyte detection. In ratiometric chemical sensors, the analyte induces changes with more than one absorption or emission band. The ratio of these bands improves the quantification and sensitivity of the chemosensor [24]. Thus, the combination of colorimetric and ratiometric fluorescence properties leads to development of active chemosensors for the sensing of toxic heavy metals in the environment and in living systems.

At present, the construction of effective colorimetric and ratiometric fluorescence chemosensor is of great need due to their simplicity and easy operation [25]. Nevertheless, most of the available chemosensors are active in the emission mode, though they do not induce any colorimetric or ratiometric response towards specific analytes. In addition, the higher selectivity of these chemosensors is restricted with other alkaline earth metal ions [26,27]. Therefore, with the essential need of the colorimetric and ratiometric fluorescence performance of the sensing probes in mind, we fabricated and report the new chemosensor 4-((3-(octadecylthio)-1,4-dioxo-1,4-dihydronaphthalen-2-yl)amino)benzenesulfonamide (**4DBS**) for the colorimetric and ratiometric fluorescence detection of Hg^{2+} in DMSO- H_2O (9:1, v/v) solution. The present chemosensor **4DBS** showed good performance in terms of high selectivity, low detection limit (LOD), high binding constant value, and negligible interference from other analytes. The coordination mechanism in the **4DBS**- Hg^{2+} complex was confirmed by FT-IR and ^1H NMR analyses. Furthermore, quantum chemical calculations were performed to support the proposed binding mechanism. Subsequent intracellular detection of Hg^{2+} in living cells and zebrafish larvae was performed. The chemosensor **4DBS** showed discriminative detection of Hg^{2+} in cancer cells that helped to distinguish human cancer cells from normal live cells.

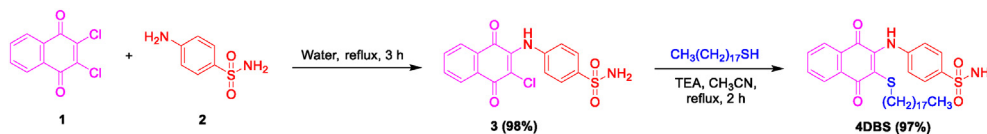
2. Experimental section

2.1. Synthesis of chemosensor **4DBS**

The chemosensor **4DBS** was synthesized according to our previously reported synthetic procedures with necessary modifications (Scheme 1) [28]. The preparation and the spectral analysis of compound **3** is accessible in our earlier investigation [29]. All synthetic procedures and the structural characterization of the chemosensor **4DBS** are briefly described in the supporting information section (SI) (Figs. S1 and S2).

2.2. Preparation of **4DBS** and metal ion stock solutions

A stock solution of 2.0×10^{-3} M **4DBS** was prepared by mixing of 0.0122 g of **4DBS** in 10 mL of DMSO. 1.0×10^{-1} M alkaline earth cations, amino acids and peptides were prepared in deionized water. Tetrabutyl ammonium salts of anions were prepared in acetonitrile (CH_3CN). From the prepared stock solutions, 25 μL **4DBS** and 50 μL analytes were diluted with 4 mL of DMSO- H_2O (9:1, v/v) solution to obtain a final concentration of 1.25×10^{-5} M and 1.25×10^{-3} M, respectively. The prepared solutions were investigated for their binding properties at ambient temperature (RT).



Scheme 1. Synthetic pathways for the preparation of chemosensor **4DBS**.

2.3. **4DBS**– Hg^{2+} complex preparation for FT-IR analysis

The ligand **4DBS** (0.076 g, 0.0025 M) and mercury(II) acetate (0.039 g, 0.0025 M) were mixed in CH_3CN (50 mL). The obtained mixture was stirred at RT for 3 h. After stirring, the resulting precipitate was isolated, washed with CH_3CN (100 mL), and dried in a hot air oven at 45 °C. The isolated organic metal complex was analyzed by FT-IR.

2.4. *In vitro* cytotoxicity assay of **4DBS**

Mouse fibroblast cells (L929) and human breast cancer cells (MCF-7) were maintained in DMEM medium with 10% FBS and 1% Pen/Strep. (Hyclone, USA). After reaching a subsequent monolayer confluency of cells with a density of 30,000 cells per well, both cell lines were incubated for 24 h with different concentrations of chemosensor **4DBS** from 0.0975 μM to 100 μM (11 doses, dissolved in DMSO). The incubated cells were treated with 10% CCK-8 solution (Dojindo Laboratories, Japan), and the cells were further incubated for another 3 h. Finally, OD values were measured at 450 nm (Microplate reader, Tecan, Austria). All cytotoxicity experiments were carried out in triplicate [30].

2.5. Bioimaging in live cells

Before bioimaging studies with L929 and MCF-7 cells, the cells were cultured in a 24-well plate for 24 h with 5% CO_2 at 37 °C. Initially, both cell lines were treated with either 6.25 μM Hg^{2+} or **4DBS** for 10 min, and the images were recorded. Next, the cells were incubated with both 6.25 μM Hg^{2+} and **4DBS**. In each incubation step, the cells were washed three times with 1X phosphate-buffered saline (PBS, pH = 7.4) to eliminate traces of unreacted Hg^{2+} and **4DBS**. The Hg^{2+} and **4DBS** incubated cells were fixed with paraformaldehyde solution (4% in PBS). Finally, images of the L929 and MCF-7 cells were captured by fluorescence microscopy under green (excitation at 490 nm; emission at 550 nm) and red (excitation at 597 nm; emission at 657 nm) channels (ECLIPSE Ts2-FL, Nikon). The quantitative amounts of fluorescence emission from live cells were measured using ImageJ software [31].

2.6. Bioimaging in zebrafish larvae

5-day-old zebrafish larvae were cultured and maintained at 28 °C in E3 medium. First, the zebrafish larvae were incubated with a water solution of 6.25 μM Hg^{2+} for 30 min and washed with 1X PBS (pH = 7.4). Next, Hg^{2+} treated zebrafish larvae were incubated with 6.25 μM **4DBS** for 30 min and subsequently washed with 1X PBS. After completion of the treatment with Hg^{2+} and **4DBS**, the fluorescence emission of the zebrafish larvae were captured by confocal microscopy (Carl Zeiss, Germany, LSM 510 META) under green channel (excitation at 554 nm; emission at 578 nm) and red channel (excitation at 625 nm; emission at 663 nm) at the Center for University-Wide Research Facilities (CURF) at Jeonbuk National University (JbNU, Jeonju, South Korea) [32].

3. Results and discussion

3.1. Design and preparation of the chemosensor **4DBS**

According to Pearson's hard–soft acid–base theory, sulfur and nitrogen binding sites are more preferable moieties for selective recognition of the soft heavy metal Hg^{2+} [33,34]. Moreover, Hg^{2+} ion is a strong electrophilic metal; thus, it would preferably be attracted by the electronegative functional group –NH in the ligand. Considering the characteristics of Hg^{2+} ion, we rationally designed and synthesized the chemosensor **4DBS** by employing simple and effective synthetic methods. First, equal stoichiometric amounts of starting materials 2,3-dichloro-1,4-naphthoquinone (**1**) and *p*-aminobenzenesulfonamide (**2**) were dispersed in water. Through the Michael-like addition reaction, compound **3** was isolated in good yield. Compound **3** was further modified with the introduction of a long aliphatic hydrocarbon chain containing a sulfur atom. The nucleophilic substitution reaction was performed between compound **3** and 1-octadecanethiol in CH_3CN with triethylamine (TEA), which gave the preferred chemosensor **4DBS** in good yield (Scheme 1).

3.2. Colorimetric detection of Hg^{2+} by **4DBS**

The colorimetric detection ability of the chemosensor **4DBS** was investigated in DMSO– H_2O (9:1, v/v) solution. Several metal cations, anions, amino acids and peptides such as Cs^+ , K^+ , Li^+ , Ag^+ , Na^+ , Mn^{2+} , Cd^{2+} , Hg^{2+} , Mg^{2+} , Ba^{2+} , Ni^{2+} , Ca^{2+} , Co^{2+} , Zn^{2+} , Sr^{2+} , Al^{3+} , La^{3+} , Br^- , Cl^- , ClO_4^- , OAc^- , NO_3^- , F^- , PO_4^- , BF_4^- , *N*-acetyl glycine (Ac-Gly-OH), *N*-acetyl glycine (Ac-Gly-OH), *L*-glutamine (*L*-Gln), *L*-(+)-2-aminobutyric acid (*L*-ABA), *N*-acetyl-*L*-methionine (Ac-*L*-Met-OH), *L*-methionine (Met), *L*-glutathione reduced (GSH), *S*-acetyl glutathione (*S*-A-GSH), *S*-hexylglutathione (*S*-Hexyl-GSH), glutathione ethyl ester (GSH-MEE), and *L*-glutathione oxidized (GSSG) was introduced into a solution containing **4DBS**. No color change was perceived for the screened analytes except for Hg^{2+} . A significant color change was obtained for the chemosensor **4DBS** with the addition of Hg^{2+} from light maroon to pale yellow in DMSO– H_2O (9:1, v/v) solution. The obtained color change was due to deprotonation or dissociation of protons in the chemosensor **4DBS**. Additionally, the obtained intramolecular charge transfer (ICT) effect in the **4DBS** – Hg^{2+} complex was another rationale for the color transformation (Fig. 1) [35].

3.3. Ratiometric fluorescence investigation of **4DBS** towards different analytes

Initially, the absorption behavior of **4DBS** (1.25×10^{-5} M) was investigated in various solvents with an added amount of water (9:1, v/v) to find a suitable solvent medium for fluorescence emission studies. Two absorption maxima were observed for the chemosensor **4DBS** at 297 nm and 514 nm from π – π^* and *n*– π^* transition states. The absorption behavior of **4DBS** was studied in various solvents; DMSO– H_2O (9:1, v/v) showed the fine absorption spectrum with high solubility of the ligand **4DBS** (Fig. S3). Next, the effect of fluorescence emission at different excitation wavelengths was examined to determine a suitable excitation wavelength for

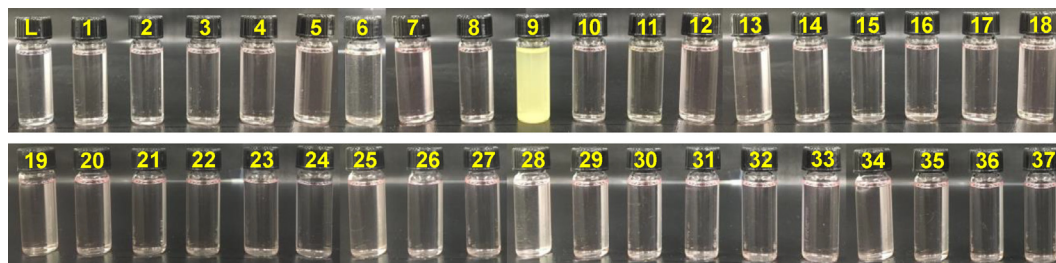


Fig. 1. “Naked-eye” investigation of **4DBS** (1.25×10^{-5} M) with the addition of different analytes (1.25×10^{-3} M) in DMSO–H₂O (9:1, v/v) solution; where L: **4DBS**, 1: Cs⁺, 2: K⁺, 3: Li⁺, 4: Ag⁺, 5: Na⁺, 6: Cu²⁺, 7: Mn²⁺, 8: Cd²⁺, 9: Hg²⁺, 10: Mg²⁺, 11: Ba²⁺, 12: Ni²⁺, 13: Ca²⁺, 14: Co²⁺, 15: Zn²⁺, 16: Sr²⁺, 17: Al³⁺, 18: La³⁺, 19: Br⁻, 20: Cl⁻, 21: ClO₄⁻, 22: OAc⁻, 23: NO₃⁻, 24: F⁻, 25: PO₄⁻, 26: BF₄⁻, 27: Ac-Gly-OH, 28: Ac-GLN-OH, 29: L-Gln, 30: L-ABA, 31: Ac-L-Met-OH, 32: Met, 33: GSH, 34: S-A-GSH, 35: S-Hexyl-GSH, 36: GSH-MEE, 37: GSSG.

fluorescence metal ion selectivity studies. While increasing the excitation wavelength from 270 nm to 300 nm, the emission intensity gradually decreased. The maximum emission intensity was obtained at an excitation wavelength of 270 nm (Fig. S4). Thus, based on the high solubility of the chemosensor **4DBS** in DMSO–H₂O (9:1, v/v) and the obtained high emission intensity from excitation at 270 nm, these parameters were selected for further fluorescence emission investigations. First, the analytes binding study of **4DBS** was performed in the presence of various metal cations, anions, amino acids and peptides including Cs⁺, K⁺, Li⁺, Ag⁺, Na⁺, Mn²⁺, Cd²⁺, Mg²⁺, Ba²⁺, Ni²⁺, Ca²⁺, Co²⁺, Zn²⁺, Sr²⁺, Al³⁺, La³⁺, Br⁻, Cl⁻, ClO₄⁻, OAc⁻, NO₃⁻, F⁻, PO₄⁻, BF₄⁻, Ac-Gly-OH, Ac-GLN-OH, L-Gln, L-ABA, Ac-L-Met-OH, Met, GSH, S-A-GSH, S-Hexyl-GSH, GSH-MEE, and GSSG. With the addition of various analytes into the **4DBS** solution, no characteristic change in fluorescence or peak shift was obtained. Interestingly, a huge peak shift was obtained with the addition of Hg²⁺ into **4DBS** solution through the fluorescence turn-on mode. Insignificant peak shifts were noticed for added analytes in **4DBS** solution; nevertheless, a red-shifted emission peak was observed with Hg²⁺. A small amount of fluorescence quenching was observed for Cu²⁺ which was due to their strong quenching and paramagnetic characters [36]. The peak at 330 nm decreased and a new emission peak appeared at 470 nm due to the ICT effect, which confirms the ratiometric character of the chemosensor **4DBS** (Fig. 2). Furthermore, the obtained ICT effect was experimentally verified by carried out UV/vis titration analysis. Well-defined absorption peaks were obtained for **4DBS** at 252, 297 and 514 nm. Upon addition of Hg²⁺ from 0 to 50 equiv. to **4DBS** solution, huge shifts were obtained in the peak positions. Red-shifted peaks were obtained from 252 to 257 nm, whereas, blue-shifted peaks were obtained from 297 to 290 nm and 514 to 487 nm (Fig S5). In addition, a good linear relationship curve was obtained for the titration analysis ($R^2 = 0.9952$, Fig. S6). Moreover, the ICT effect was further evaluated by the plot of Stokes shift (in wavenumber) against solvent orientation polarizability (Δf) which was calculated from a Lippert–Mataga equation ($\Delta f = (\epsilon - 1) / (2\epsilon + 1) - (n^2 - 1) / (2n^2 + 1)$), where ϵ is the dielectric constant and n is the refractive index of the solvent [37]. All the spectral data of **4DBS** and its Hg²⁺ complex were presented in Table S1. From the attained results, it was observed that the **4DBS**–Hg²⁺ complex show ICT effect in CH₃CN, MeOH and DMSO by shifting their Stokes shifts non-linearly with the increment of Δf value (Fig. S7). Also, the positive values representing that the excited state of the molecules are more polar in comparison to the ground state. Hence, these results indicate that the ICT effect was obtained between the **4DBS** – Hg²⁺ complex which induced the enhanced ratiometric fluorescence emission. Likewise, the obtained higher selectivity with enhanced fluorescence emission intensity could be reasonably justified as follows. According to Pearson’s hard-soft acid-base theory, secondary amine (–NH) is a soft base and Hg²⁺ is a soft

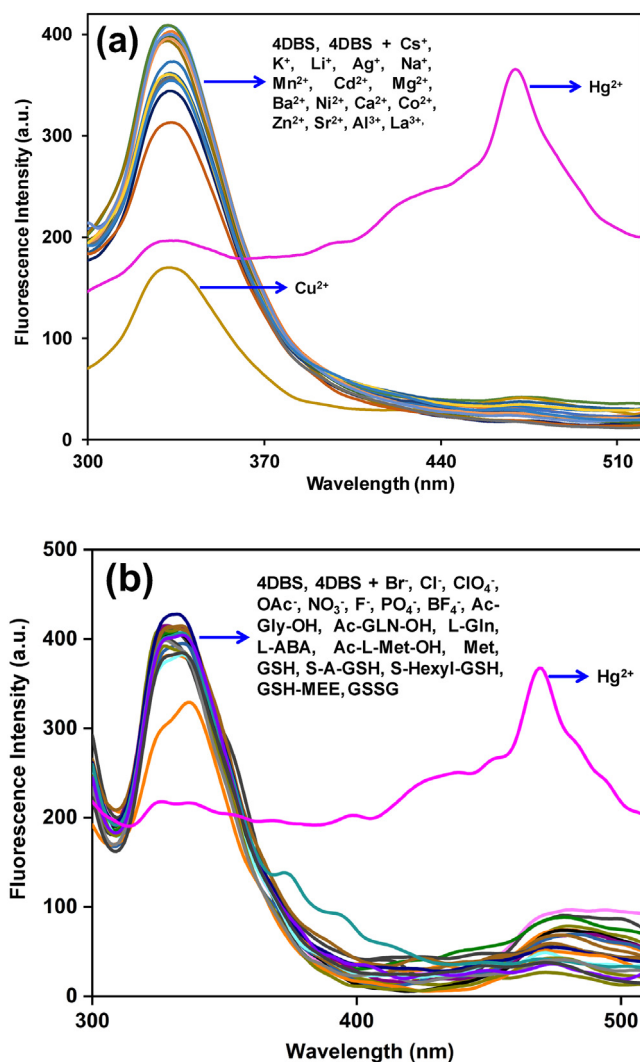


Fig. 2. Selectivity study of **4DBS** (1.25×10^{-5} M) upon addition of different analytes (1.25×10^{-3} M) in DMSO–H₂O (9:1, v/v) solution. (a) Selectivity study of **4DBS** with various metal ions. (b) Selectivity study of **4DBS** with various anions, amino acids and peptides, $\lambda_{\text{ex}} = 270$ nm.

acid. Thus, Hg²⁺ would preferably establish its coordinate bond with secondary amine (–NH) in **4DBS** with a ratiometric fluorescence signal [38]. Also, the induced excitation energy transfer of –NH to free d orbitals of Hg²⁺ improves good selectivity/emission behaviors [39]. Another most significant reason is the hydrogen bonding interaction between **4DBS** and Hg²⁺ that enhances better fluorescence performance. Concerning the IUPAC rule, the higher

electrophilic nature of Hg^{2+} perfectly interacts through the hydrogen bonding with the high electronegative $-\text{NH}$ group [31]. Thus, because of the high nucleophilicity of fluorophore ($-\text{NH}$), and electrophilicity of Hg^{2+} coordinated through the suitable way, **4DBS** showed good selectivity with higher ratiometric fluorescence emission signal for Hg^{2+} over the other analytes investigated. The effect of water on the **4DBS** – Hg^{2+} system was investigated by increasing the quantity of water in DMSO solution of **4DBS**. The results revealed that the maximum fluorescence intensity was obtained with a 10% water fraction. The emission intensity was significantly reduced upon addition of 20–100% water. In addition, the fluorescence emission intensity was considerably reduced with the addition of 20 mM HEPES buffer solution (pH = 7.5) in DMSO– H_2O (9:1, v/v) solution (Fig. S8). Moreover, the effect of solvents for the **4DBS** – Hg^{2+} complex in various solvents was investigated. Among various solvents, the solvents such as CH_3CN , MeOH and DMSO were exhibited higher fluorescence emission intensities, nevertheless, poor linear relationship curves were obtained for CH_3CN ($R^2 = 0.4833$), and MeOH ($R^2 = 0.8755$) (Figs. S9–S11). Therefore, DMSO– H_2O (9:1, v/v) solvent system is a more feasible sensing medium for the chemosensor **4DBS** for the detection of Hg^{2+} ion.

Next, a fluorescence titration experiment was performed to evaluate the stability of the complex with increasing amounts of Hg^{2+} in **4DBS** solution. Upon excitation at 270 nm, with increasing concentrations of Hg^{2+} in **4DBS** solution, the emission intensity at 330 nm gradually decreased and a new red-shifted emission peak at 470 nm gradually developed with a good linear relationship curve (Fig. S12, $R^2 = 0.9896$). A well-shaped isoemission point was observed at 366 nm, which indicates formation of the **4DBS** – Hg^{2+} complex [40]. Fluorescence spectral changes were stopped after the addition of 100 equiv. of Hg^{2+} in **4DBS** solution (Fig. 3), which was the maximum saturation level of **4DBS** solution. This fluorescence titration study indicates that the chemosensor **4DBS** could be employed in the quantitative determination of Hg^{2+} in environmental and biological samples. Furthermore, the selectivity and influence of other metal ions, anions, amino acids and peptides on the **4DBS** – Hg^{2+} complex were examined. As presented in Fig. 4, the competitive study indicated that the presence of other analytes showed zero or negligible interference in the detection of Hg^{2+} , and the ratio of the ratiometric spectral changes was not disrupted by the other metals, anions, amino acids and peptides. These findings reveal that the chemosensor **4DBS** distin-

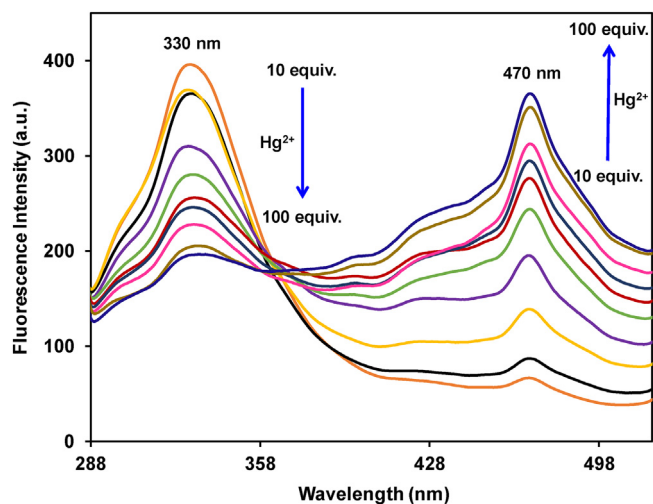


Fig. 3. Fluorescence titration analysis of **4DBS** (1.25×10^{-5} M) with the increased amount of Hg^{2+} (1.25×10^{-4} M to 1.25×10^{-3} M) in DMSO– H_2O (9:1, v/v) solution, $\lambda_{\text{ex}} = 270$ nm.

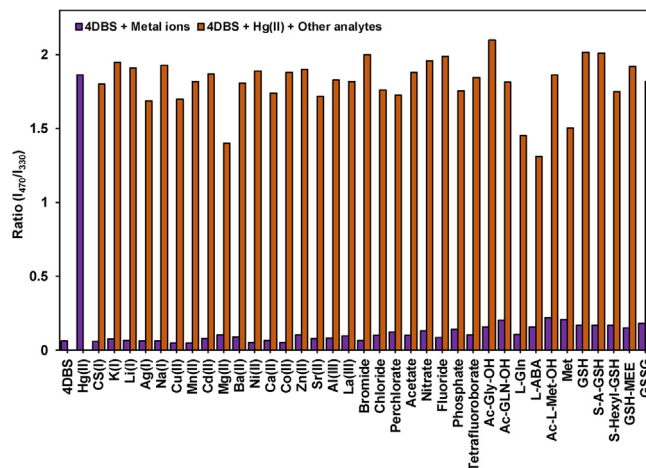


Fig. 4. The analytes competitive study of **4DBS** (1.25×10^{-5} M) with Hg^{2+} (1.25×10^{-3} M) and co-existing with other metal cations, anions, amino acids and peptides (1.25×10^{-3} M) in DMSO– H_2O (9:1, v/v) solution, $\lambda_{\text{ex}} = 270$ nm.

guished Hg^{2+} from other chemically related analytes, in particular Ag^+ , which is the most interactive metal ion in several chemosensors [41].

3.4. Evaluation of binding stoichiometry and limit of detection (LOD)

A Job's plot analysis was employed to evaluate the binding stoichiometry of the **4DBS**– Hg^{2+} complex from the fluorescence intensity ratio (I_{470}/I_{330}) [42]. With increasing addition of Hg^{2+} into **4DBS** solution, the ratio of the fluorescence intensity consistently increased; whereas, the ratio of the emission intensity decreased after 0.5-mole fraction. The obtained Job's plot analysis indicates that a 1:1 coordination stoichiometry was obtained in the **4DBS**– Hg^{2+} complex (Fig. S13). Next, from the Benesi-Hildebrand plot, the association constant (K_s) was determined based on the ratio of the fluorescence titration analysis. The determined K_s value for the **4DBS**– Hg^{2+} system was $K_s = 5.55 \times 10^2 \text{ M}^{-1}$ (Fig. S14). The LOD of **4DBS** towards Hg^{2+} was calculated to be $0.451 \mu\text{M}$ from the formula $3\sigma/k$ [43] where, σ = standard deviation and k = slope value.

3.5. The reversibility of the chemosensor **4DBS** towards Hg^{2+}

Reversibility of the chemosensor is a key feature, which can be extensively utilized in the finding of selective analytes [44]. Thus, the reversibility of the chemosensor **4DBS** was investigated with the chelating agent EDTA. As expected, the addition of EDTA to the **4DBS** and Hg^{2+} mixture resulted in a decrease in the fluorescence intensity at 470 nm and a concurrent increase in the fluorescence intensity at 330 nm. The fluorescence intensity at 470 nm could be regenerated upon further addition of Hg^{2+} (Fig. 5). Regeneration and reversibility are significant properties in the development of novel chemical sensing probes, and these results suggest that the present chemosensor **4DBS** could be utilized in real time analysis.

3.6. Effect of pH

To utilize the chemosensor for various applications, the effect of fluorescence under different pH (from 1 to 13) for **4DBS** and the **4DBS**– Hg^{2+} complex were investigated in DMSO– H_2O (9:1, v/v) solution. From the obtained results, **4DBS** showed weaker emission intensity for the entire pH window and continue unchanged. Interestingly, with the addition of Hg^{2+} to **4DBS** solution, the intensified

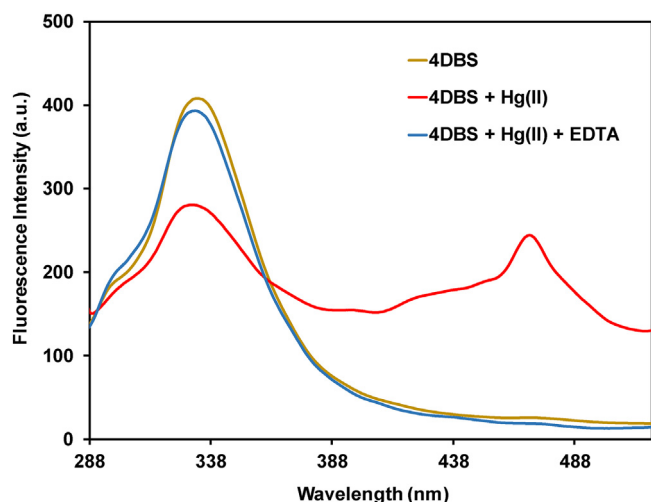


Fig. 5. Chemosensor reversibility analysis of **4DBS** (1.25×10^{-5} M) with Hg^{2+} (6.25×10^{-4} M) and EDTA (2.5×10^{-3} M) in DMSO- H_2O (9:1, v/v) solution, $\lambda_{\text{ex}} = 270$ nm.

fluorescence signals were obtained from pH 9–13. Nevertheless, poor fluorescence emissions were received over the pH of 1–8 (Fig. S15). Under acidic and neutral conditions, because of the functional group's protonation in **4DBS**, the fluorescence emission intensity was hindered in **4DBS**- Hg^{2+} complex, nevertheless, in extremely basic environments, the hydrolysis of Hg^{2+} to form $\text{Hg}(\text{OH})_2$ which induced the enhanced fluorescence emissions [45]. Thus, the obtained results indicate that the chemosensor **4DBS** could be utilized to monitor Hg^{2+} under extreme basic pH conditions.

3.7. FT-IR analysis of **4DBS**- Hg^{2+} complex

Initially, to determine the binding mode of the chemosensor **4DBS** towards Hg^{2+} , IR spectra for Hg^{2+} , **4DBS**, and the **4DBS**- Hg^{2+} complex were examined. All of the measured FT-IR spectra are given in Fig. 6. From the obtained IR signals, sharp stretching vibrational signals were obtained at 3261 cm^{-1} and 3308 cm^{-1} for the $-\text{NH}_2$ group of the chemosensor **4DBS**. A clear well-defined IR signal was observed at 3357 cm^{-1} for the $-\text{NH}$ group of the probe. In the FT-IR spectrum of the **4DBS**- Hg^{2+} complex, the $-\text{NH}$ signal at 3357 cm^{-1} completely disappeared. The $-\text{NH}_2$ stretching vibrational signals broadened and appeared at 3274 cm^{-1} due to the induced electronic effects between the chemosensor and the metal ion [46]. None of the signals from the other functional groups were altered because of the coordination in the metal complex. From these results, it could be inferred that the coordination binding was established for Hg^{2+} with the $-\text{NH}$ group in **4DBS**. This coordination behavior could be justified according to Pearson's acid-base theory. The electrophilic nature of the soft heavy metal Hg^{2+} specifically preferred to bind with the nucleophilic nitrogen atom in the chemosensor **4DBS** [38]. Thus, these findings showed that the coordination of Hg^{2+} mainly occurred with the $-\text{NH}$ group of **4DBS**.

3.8. ^1H NMR titration analysis

To provide a deeper analysis of participation of the functional groups in the **4DBS**- Hg^{2+} complex, ^1H NMR titration analysis was undertaken with the absence and presence of Hg^{2+} in **4DBS** solution. In a typical titration experiment, Hg^{2+} was gradually added to the solution of **4DBS** (3.0 mg, 10 mmol) in DMSO d_6 . As presented in Fig. 7a, a sharp signal appeared for the secondary amine ($-\text{NH}$) of

4DBS at 9.2822 ppm. Upon initial addition of 0.2 equiv. of Hg^{2+} in **4DBS** solution, the intensity of the $-\text{NH}$ signal at 9.2822 ppm slightly decreased. Moreover, with further addition of Hg^{2+} into **4DBS** solution, the signal for the $-\text{NH}$ group became less sharp and the peak intensity gradually decreased without any position shift. No further changes were perceived after the addition of 0.8 equiv. of Hg^{2+} , which indicates that the **4DBS** solution reached its maximum saturation point and the obtained metal complex ratio was 1:1. No other significant changes were obtained from the NMR signals of the other aromatic and aliphatic moieties of **4DBS**. In addition, the hydrolytic stability of the **4DBS**- Hg^{2+} complex in DMSO d_6 - D_2O (9:1, v/v) was investigated. As presented in Fig. 7b, the peaks for primary ($-\text{NH}_2$) and secondary amines ($-\text{NH}$) were disappeared at 7.1784 and 9.1992 ppm, respectively, without the presence of Hg^{2+} . The disappearance of the peaks occurred because of the exchange of protons from D_2O to **4DBS**. However, with the addition of 0.2 equiv. Hg^{2+} , the considerable amount of proton signal for primary amine ($-\text{NH}_2$) at 7.1784 ppm was regenerated due to the coordination of Hg^{2+} with secondary amine ($-\text{NH}$). For the entire titration analysis, the peak at 9.1992 ppm remains unchanged which indicates the obtained possible coordination mechanism between secondary amine ($-\text{NH}$) in **4DBS** and Hg^{2+} . Furthermore, the hydrolytic stability of the coordination complex was investigated at different time intervals (Figs. S16 and S17). The observed results indicate that the coordination complex was highly stable even after 6 h. Additionally, the temperature effect on the complex was investigated. At 60°C , the protons for primary ($-\text{NH}_2$) and secondary amines ($-\text{NH}$) were exchanged with D_2O and their respective signals were disappeared, whereas, the remaining aromatic and aliphatic proton signals were kept unchanged (Fig. S18). Thus, these results confirm that the secondary amine ($-\text{NH}$) in **4DBS** was involved in the coordination mechanism with Hg^{2+} . Also, these combined titration analyses in the aqueous DMSO revealed that the **4DBS** and its Hg^{2+} complex were highly stable under different experimental conditions.

3.9. Electrochemical measurements

The naphthoquinone derivatives were electroactive, underwent redox processes [47]. To confirm the coordination binding between the chemosensor **4DBS** and Hg^{2+} , the electrochemical measurement was carried out by employing cyclic voltammetry (CV). 0.1 M Tetra-butylammonium tetrafluoroborate (TBATFB, dissolved in CH_3CN) was used as a supporting electrolyte medium with a scan rate of 100 mV s^{-1} [48]. The redox potential (E_{redox}) values were calculated by employing the midpoint peak potentials. First, the CV of **4DBS** was measured, and well-formed anodic and cathodic peaks appeared at -1.142 , -0.922 , and -1.354 , -1.025 V, respectively. Though, the reduction potentials of the **4DBS**- Hg^{2+} complex was shifted to the anodic region due to the electron-donating character of the amino-phenyl moiety linked to naphthoquinone. The respective anodic and cathodic peaks were obtained at 0.289, -0.078 and -1.069 , -0.371 V, respectively (Fig. S19). It has been noticed that the chemosensor and its Hg^{2+} complex displays a reversible reduction reaction to form semiquinone radical and finally, semiquinone radical fully reduced to its corresponding hydroquinone ($\text{Q}/\text{SQ}^{\cdot-}/\text{H}_2\text{Q}$, Eqs. 1–3). Constructed on the redox potential, the reduction ability of **4DBS** and its Hg^{2+} complex was determined (Table S2). The calculated redox potentials indicate that **4DBS** was easily reduced than the **4DBS**- Hg^{2+} complex because of occurred ICT effect between **4DBS** and Hg^{2+} . Furthermore, the CV studies of **4DBS** and **4DBS**- Hg^{2+} complex were investigated in the DMSO medium (Fig. S20). Well-defined redox peaks have appeared for the systems, however, their reduction potential is comparatively lower than that of CV analysis of **4DBS** and its Hg^{2+} complex in CH_3CN . This may be because of the less acidity of CH_3CN ($\text{pK}_a = 25$) than

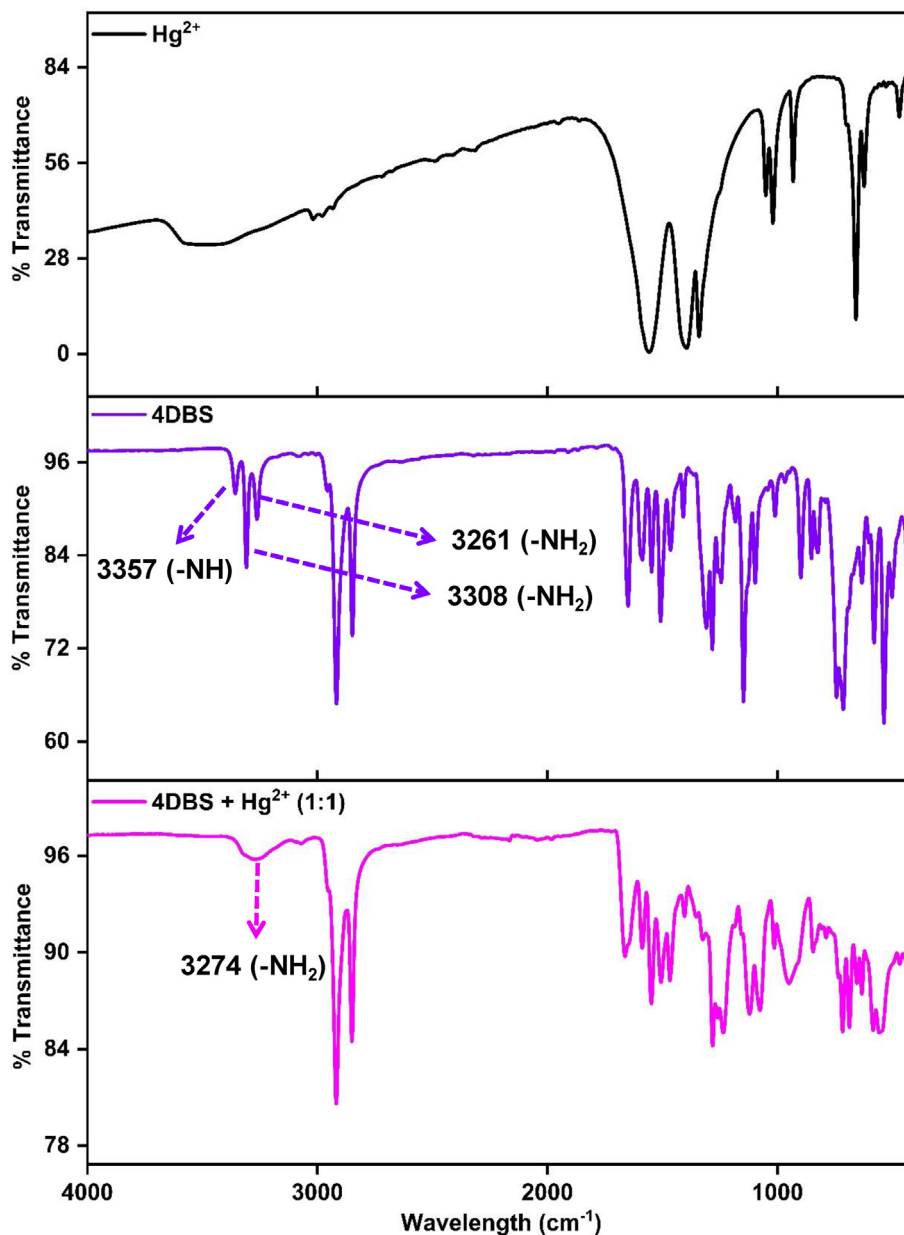


Fig. 6. FT-IR analysis of $\text{Hg}(\text{OAc})_2$, **4DBS** and **4DBS**- Hg^{2+} complex.

DMSO ($\text{pK}_a = 35$) which could be easily provided the protons to make the feasible reduction reaction [49]. This comparative study is indicative of the reduction reaction in the DMSO medium were not a diffusion-controlled process. Therefore, these electrochemical analyses confirmed a strong binding affinity was obtained between the chemosensor **4DBS** and Hg^{2+} .



3.10. Quantum chemical calculations (DFT)

To verify the electronic character of **4DBS** and its Hg^{2+} complex, theoretical calculations (DFT) were performed with the B3LYP

method along with the LANL2DZ basis set using the Gaussian 09 software package [50]. The optimized structure of **4DBS** showed the naphthoquinone and octadecanethiol moieties to be approximately in the same plane. However, the sulfonamide moiety was slightly twisted from the naphthoquinone unit. Moreover, in the optimized geometry of the **4DBS**- Hg^{2+} system, Hg^{2+} made a coordination bond with the -NH group through a hydrogen bonding interaction with a bond distance of 2.40 Å (Fig. S21). As shown in Fig. 8, the free **4DBS** exhibited an energy distribution at LUMO and HOMO energy levels similar to the naphthoquinone unit with an energy value of 1.831 eV. Upon coordination of **4DBS** with Hg^{2+} , the energy distribution at the LUMO and HOMO energy levels completely migrated to the sulfonamide and octadecanethiol units with an energy value of 0.171 eV. In addition, the energy of the **4DBS**- Hg^{2+} complex was significantly decreased in comparison with that of the free **4DBS**, which indicates formation of a stable coordination complex with an energy difference of 1.66 eV. These results suggest that the binding of Hg^{2+} with the

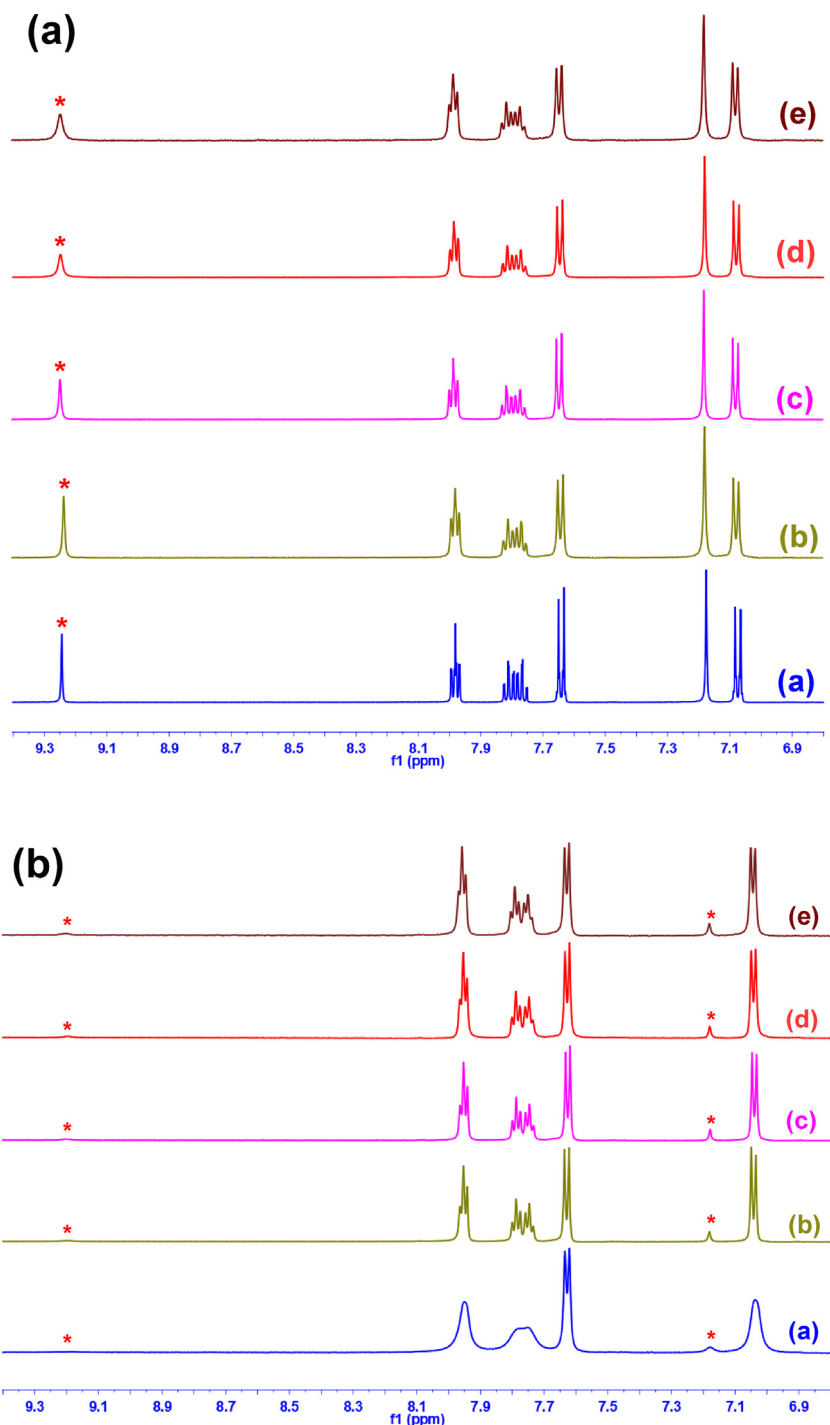


Fig. 7. (a) ^1H NMR analysis of **4DBS** with (a) 0.0 (b) 0.2 (c) 0.4 (d) 0.6 (e) 0.8 equivalents of Hg^{2+} in $\text{DMSO } d_6$ at 0 h. (b) ^1H NMR analysis of **4DBS** with (a) 0.0 (b) 0.2 (c) 0.4 (d) 0.6 (e) 0.8 equivalents of Hg^{2+} in $\text{DMSO } d_6\text{-D}_2\text{O}$ (9:1, v/v) at 0 h.

naphthoquinone-sulfonamide moiety promotes the ICT effect *via* enhancing the electron-withdrawing capacity of the $-\text{NH}$ group. This phenomenon induced the ratiometric turn-on response towards Hg^{2+} with a red-shift in the emission spectrum [51].

Moreover, the excited state properties of **4DBS** and its Hg^{2+} complex were investigated by the TD-DFT method (Fig. S22). The chemosensor **4DBS** shows the excitation and emission peaks at 216, 250, 338, 440 nm and 408, 434, 461, 479, 513, 541, 590, 690 nm, respectively, that corresponds to the highest energy of 5.93 eV and 3.02 eV. The excitation and emission spectra calcu-

tions were executed with an energy limit of 8.00 eV (Fig. S22a). Upon addition of Hg^{2+} to the chemosensor **4DBS**, that induced the changes in the structural and transition states at different level which resulted in emission at various ranges. The excitation spectra of the **4DBS**- Hg^{2+} complex display peaks at 222, 238, 247, 262, 309 and 326 nm. The emission spectra show intense peaks at 157, 183, 232 and 342 nm that corresponds to the highest energy of 7.68 eV and 7.88 eV (Fig. S22b). The fluorescence shift was calculated from the excitation-emission spectra that demonstrate the transitions from green-blue which is

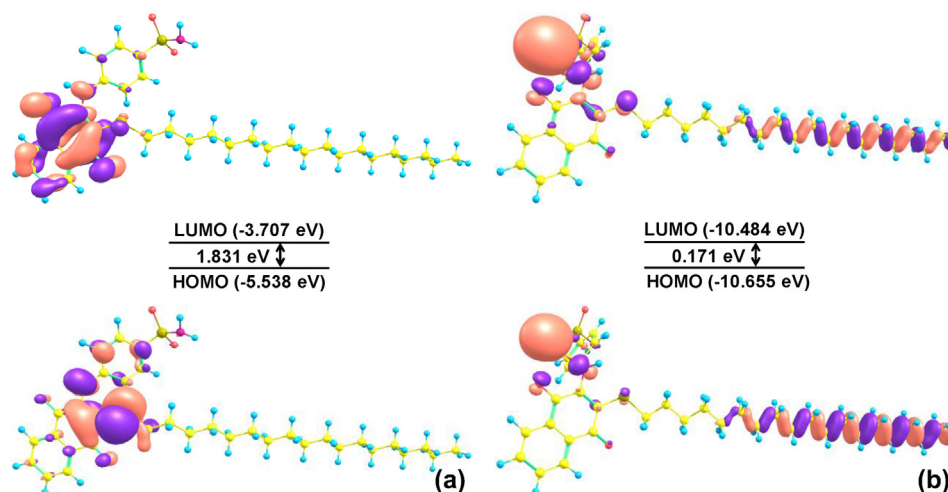


Fig. 8. The LUMO and HOMO energy levels of 4DBS (a) and 4DBS-Hg²⁺ system (b).

consistent with the color changes observed from the colorimetric experiment (Fig. S22c,d). The experiment shows a transformation of color from light maroon to pale yellow, the peaks were shifted from a higher wavelength to a lower wavelength which in agreement with the DFT calculations. Likewise, the natural transition orbital (NTO) analysis was carried out to understand the distribution of photogenerated holes and electron density of the 4DBS and 4DBS-Hg²⁺ complex. The NTO calculations were performed up to the 12th excited state and the distribution for 4DBS which exhibit the transition from the tail region to the center of the chemosensor. However, with the addition of Hg²⁺ to 4DBS, the wave function of 4DBS was modified and the electron density distribution was perceived around Hg²⁺ ion (Figs. S23 and S24). These energy transfer may happen because of the interaction of Hg²⁺ with the chemosensor 4DBS. These changes in the energy distribution indicate the structural changes made by the metal binding with the chemosensor, which resulted in the observed color change and the ratiometric fluorescence behavior. These discussions are more consistent with the proposed coordination mechanism of 4DBS for Hg²⁺ detection (Scheme 2).

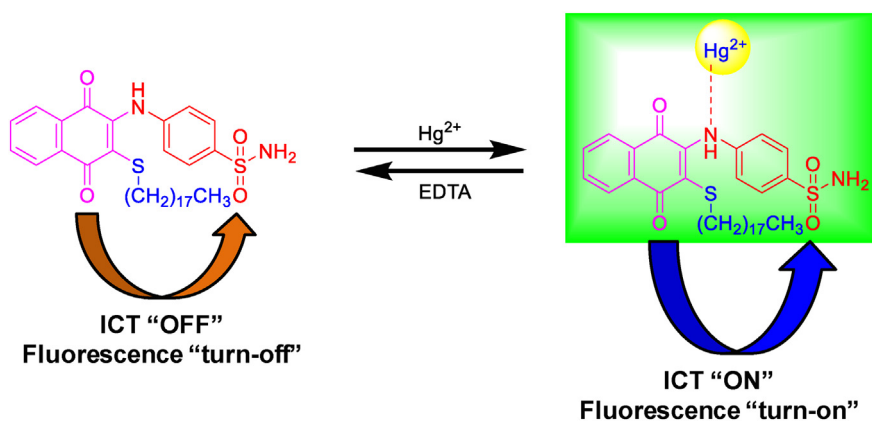
3.11. Bioimaging investigations

3.11.1. Discriminative identification of Hg²⁺ in live cells

To investigate the efficiency of the chemosensor 4DBS in biological samples, bioimaging study was performed in live cells and zeb-

rafish larvae. To verify the toxicity of the chemosensor 4DBS, cell viability assay was carried out in two cell lines including the mouse fibroblast cells (L929) and human breast cancer cells (MCF-7). The obtained results revealed that the chemosensor 4DBS has a very weak or negligible toxicity effect in live cells even at a higher concentration. Greater than 90% of the cells were viable in the presence of chemosensor 4DBS (Fig. S25). Hence, the present chemosensor 4DBS is biocompatible with live cells.

Based on the profound photophysical and photochemical properties of the chemosensor 4DBS for the selective detection of Hg²⁺, we were further motivated to investigate the intracellular detection of Hg²⁺ in live cells. For the intracellular analysis of the chemosensor 4DBS, L929 and MCF-7 cells were chosen for detection of Hg²⁺. From the obtained cytotoxicity analysis, two safer concentrations of 4DBS (6.25 μM and 12.5 μM) were carefully selected for the bioimaging analysis. First, Hg²⁺ and 4DBS were separately incubated with L929 and MCF-7 cells, and no fluorescence emission was observed (Figs. S26 and S27). Fascinatingly, when the L929 and MCF-7 cells were incubated with Hg²⁺ and 4DBS in a combined manner (Hg²⁺ incubated at first), a higher contrast fluorescence emission was obtained in MCF-7 cells than in L929 cells (Fig. 9). A robust fluorescence emission intensity was obtained in MCF-7 cells, which was 3.55 fold (green channel) and 6.02 fold (red channel) higher than the emission attained in L929 cells. The intensity of the fluorescence emission increased in a dose-dependent manner (Figs. S28–S30). The subcellular distribu-



Scheme 2. The proposed coordination mechanism of 4DBS towards Hg²⁺.

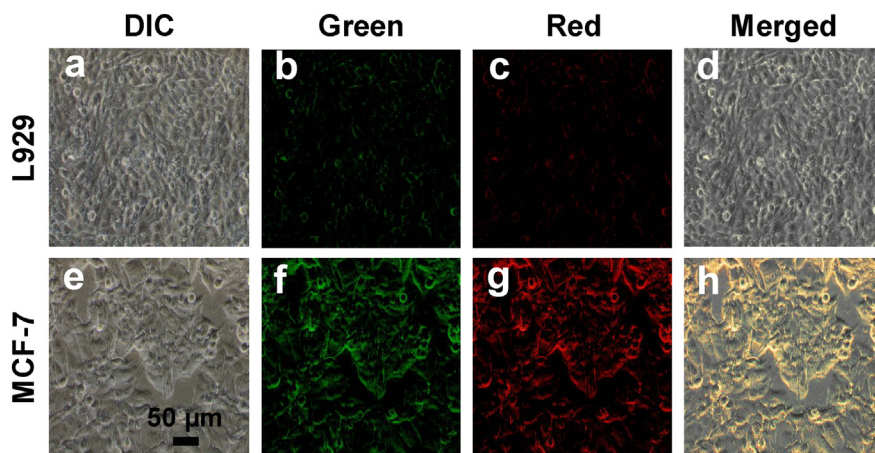


Fig. 9. Fluorescence bioimaging of Hg^{2+} in L929 and MCF-7 cells; where, a–d = L929 cells treated with $6.25 \mu\text{M}$ Hg^{2+} and **4DBS**, respectively; where, e–h = MCF-7 cells treated with $6.25 \mu\text{M}$ Hg^{2+} and **4DBS**, respectively.

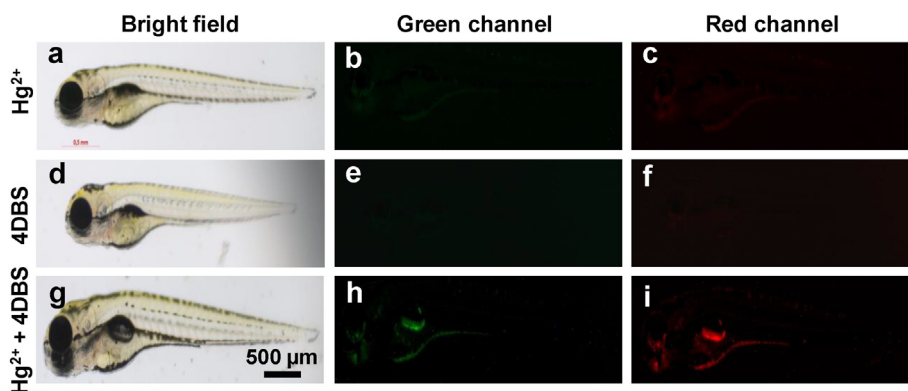


Fig. 10. Confocal fluorescence bioimaging of Hg^{2+} in zebrafish larvae; where, a–c = zebrafish larvae incubated with $6.25 \mu\text{M}$ Hg^{2+} ; d–f = zebrafish larvae incubated with $6.25 \mu\text{M}$ **4DBS**; g–i = zebrafish larvae incubated with $6.25 \mu\text{M}$ Hg^{2+} and **4DBS**, respectively.

tion of the chemosensor **4DBS** and Hg^{2+} were mainly found in the cytoplasm of the cells. The obtained results indicate that the chemosensor **4DBS** effectively detected Hg^{2+} in human cancer cells in contrast to normal live cells. Thus, it is demonstrated that the chemosensor **4DBS** has significant capacity to penetrate the cell walls and could induce discriminative tracking of Hg^{2+} in human cancer cells compared to normal cells. Moreover, the analytical parameters of recently reported chemosensors given in Table S3 which highlighted the better selectivity, sensitivity, and binding constant of the presently constructed chemosensor **4DBS**.

3.11.2. Bioimaging analysis in zebrafish larvae

Finally, we verified the sensing capability of the chemosensor **4DBS** in 5-day-old zebrafish larvae. Zebrafish larvae are well documented for *in vivo* bioimaging analysis due to their transparent nature. Besides, zebrafish larvae share about 70% of the comparable genetic assembly to humans. Hence, zebrafish larvae are a suitable animal model for the *in vivo* bioimaging analysis [52]. As given in Fig. 10, at first, zebrafish larvae were incubated with $6.25 \mu\text{M}$ Hg^{2+} for 30 min, and the images were recorded. No fluorescence emission was observed (Fig. 10a–c). Next, the zebrafish larvae were incubated with $6.25 \mu\text{M}$ **4DBS** for 30 min, and a similar fluorescence emission to the previous experiments was displayed (Fig. 10d–f). Finally, the zebrafish larvae were incubated with both $6.25 \mu\text{M}$ Hg^{2+} and **4DBS** for 30 min. Fascinatingly, enhanced fluorescence emission was obtained in both the green and red channels

(Fig. 10g–i). The obtained results indicate that the chemosensor **4DBS** has excellent tissue penetration capacity and could effectively recognized Hg^{2+} distribution in zebrafish larvae.

4. Conclusions

In conclusion, a new rationally designed naphthoquinone-based colorimetric and ratiometric fluorescence chemosensor **4DBS** was successfully synthesized and its luminescence sensing properties were investigated for Hg^{2+} . The chemosensor was shown to possess excellent selectivity, sensitivity, rapid response for Hg^{2+} (less than 2 min), and a good association constant value in DMSO– H_2O (9:1, v/v) solution. The colorimetric detection of Hg^{2+} could be expediently visualized in a direct naked-eye manner, which provided a convenient, low-cost identification of Hg^{2+} . The selectivity towards Hg^{2+} was enabled by quenching of the monomeric fluorescence emission at 330 nm with progressive red-shifted emission development of a new peak at 470 nm for ratiometric recognition. The complexometric titration studies indicate that the chemosensor was highly selective for Hg^{2+} without interference from other co-existed analytes. In addition, **4DBS** was successfully employed to track Hg^{2+} at micromolar concentrations in two different live cell lines and zebrafish larvae. Moreover, the discriminative detection of Hg^{2+} at the intracellular level in human cancer cells and normal cells were accomplished. Thus, the outcome of these results suggests **4DBS**

is a potential lead molecule for the further development of bioimaging agents in the identification of cancer cells.

Declaration of Competing Interest

The authors declare that they have no known competing financial interests or personal relationships that could have appeared to influence the work reported in this paper.

Acknowledgment

This work was supported by grants from the Medical Research Center Program (NRF-2017R1A5A2015061) through the National Research Foundation (NRF), which is funded by the Korean government (MSIP). This research was also funded by Korea Institute of Energy Technology Evaluation and Planning (KETEP) and the Ministry of Trade, Industry & Energy (MOTIE) of the Republic of Korea (No. 20184030202210).

Appendix A. Supplementary data

Supplementary data to this article can be found online at <https://doi.org/10.1016/j.saa.2021.119776>.

References

- [1] K.P. Carter, A.M. Young, A.E. Palmer, Fluorescent sensors for measuring metal ions in living systems, *Chem. Rev.* 114 (2014) 4564–4601.
- [2] Y. Zhou, J.F. Zhang, J. Yoon, Fluorescence and colorimetric chemosensors for fluoride-ion detection, *Chem. Rev.* 114 (2014) 5511–5571.
- [3] S.-H. Park, N. Kwon, J.-H. Lee, J. Yoon, I. Shin, Synthetic ratiometric fluorescent probes for detection of ions, *Chem. Soc. Rev.* 49 (2020) 143–179.
- [4] Directive 2011/65/EU of the "European Parliament and of the Council of 8 June 2011 on the restriction of the use of certain hazardous substances in electrical and electronic equipment (recast)", in.
- [5] Y. Wei, B. Li, X. Wang, Y. Duan, A nano-graphite–DNA hybrid sensor for magnified fluorescent detection of mercury(II) ions in aqueous solution, *Analyst* 139 (2014) 1618–1621.
- [6] Q. Wang, D. Kim, D.D. Dionysiou, G.A. Sorial, D. Timberlake, Sources and remediation for mercury contamination in aquatic systems—a literature review, *Environ. Pollut.* 131 (2004) 323–336.
- [7] H.-S. So, B.A. Rao, J. Hwang, K. Yesudas, Y.-A. Son, Synthesis of novel squaraine-bis(rhodamine-6G): A fluorescent chemosensor for the selective detection of Hg²⁺, *Sens. Actuators, B* 202 (2014) 779–787.
- [8] Y. Jiao, X. Liu, L. Zhou, H. He, P. Zhou, C. Duan, A Schiff-base dual emission ratiometric fluorescent chemosensor for Hg²⁺ ions and its application in cellular imaging, *Sens. Actuators, B* 247 (2017) 950–956.
- [9] G.G. Vinoth Kumar, M.P. Kesavan, A. Tamilselvi, G. Rajagopal, J.D. Raja, K. Sakthipandi, J. Rajesh, G. Sivaraman, A reversible fluorescent chemosensor for the rapid detection of Hg²⁺ in an aqueous solution: Its logic gates behavior, *Sens. Actuators, B* 273 (2018) 305–315.
- [10] Z.-X. Han, H.-Y. Luo, X.-B. Zhang, R.-M. Kong, G.-L. Shen, R.-Q. Yu, A ratiometric chemosensor for fluorescent determination of Hg²⁺ based on a new porphyrin-quinoline dyad, *Spectrochim. Acta, Part A* 72 (2009) 1084–1088.
- [11] X. Zhang, J. Yin, J. Yoon, Recent advances in development of chiral fluorescent and colorimetric sensors, *Chem. Rev.* 114 (2014) 4918–4959.
- [12] C. Wolf, Stereolabile chiral compounds: analysis by dynamic chromatography and stopped-flow methods, *Chem. Soc. Rev.* 34 (2005) 595–608.
- [13] C. Simó, C. Barbas, A. Cifuentes, Chiral electromigration methods in food analysis, *Electrophoresis* 24 (2003) 2431–2441.
- [14] A.S. Ribeiro, A.L. Moretto, M.A.Z. Arruda, S. Cadore, Analysis of powdered coffee and milk by ICP OES after sample treatment with tetramethylammonium hydroxide, *Microchim. Acta* 141 (2003) 149–155.
- [15] V. Schurig, Practice and theory of enantioselective complexation gas chromatography, *J. Chromatogr. A* 965 (2002) 315–356.
- [16] V. Subramanian, S. Lee, S. Jena, S.K. Jana, D. Ray, S.J. Kim, P. Thalappil, Enhancing the sensitivity of point-of-use electrochemical microfluidic sensors by ion concentration polarisation – A case study on arsenic, *Sens. Actuators, B* 304 (2020) 127340.
- [17] J.-B. Li, Y. Liu, X.-J. Zheng, D. Wang, An off-on chemosensor for Hg²⁺ based on the excimer emission of anthracene, *Microchem. J.* 150 (2019) 104123.
- [18] Y.-K. Yang, K.-J. Yook, J. Tae, A rhodamine-based fluorescent and colorimetric chemosensometer for the rapid detection of Hg²⁺ ions in aqueous media, *J. Am. Chem. Soc.* 127 (2005) 16760–16761.
- [19] P. Samanta, S. Let, W. Mandal, S. Dutta, S.K. Ghosh, Luminescent metal–organic frameworks (LMOFs) as potential probes for the recognition of cationic water pollutants, *Inorg. Chem. Front.* 7 (2020) 1801–1821.
- [20] M.K. Amini, B. Khezri, A.R. Firooz, Development of a highly sensitive and selective optical chemical sensor for batch and flow-through determination of mercury ion, *Sens. Actuators, B* 131 (2008) 470–478.
- [21] G. Dhaka, J. Singh, N. Kaur, Benzothiazole based chemosensors having appended amino group(s): Selective binding of Hg²⁺ ions by three related receptors, *Inorg. Chim. Acta* 462 (2017) 152–157.
- [22] R. Martínez-Máñez, F. Sancenón, Fluorogenic and chromogenic chemosensors and reagents for anions, *Chem. Rev.* 103 (2003) 4419–4476.
- [23] C. Suksai, T. Tuntulani, Chromogenic anion sensors, *Chem. Soc. Rev.* 32 (2003) 192–202.
- [24] R. Gui, H. Jin, X. Bu, Y. Fu, Z. Wang, Q. Liu, Recent advances in dual-emission ratiometric fluorescence probes for chemo/biosensing and bioimaging of biomarkers, *Coord. Chem. Rev.* 383 (2019) 82–103.
- [25] S. Mukherjee, M. Shah, K. Chaudhari, A. Jana, C. Sudhakar, P. Srikrishnarka, M.R. Islam, L. Philip, T. Pradeep, Smartphone-based fluoride-specific sensor for rapid and affordable colorimetric detection and precise quantification at sub-ppm levels for field applications, *ACS Omega* 5 (2020) 25253–25263.
- [26] A. Singh, T. Raj, T. Aree, N. Singh, Fluorescent organic nanoparticles of biginelli-based molecules: Recognition of Hg²⁺ and Cl⁻ in an aqueous medium, *Inorg. Chem.* 52 (2013) 13830–13832.
- [27] N.M.M. Moura, C. Núñez, S.M. Santos, M.A.F. Faustino, J.A.S. Cavaleiro, M.G.P.M. S. Neves, J.L. Capelo, C. Lodeiro, Synthesis, spectroscopy studies, and theoretical calculations of new fluorescent probes based on pyrazole containing porphyrins for Zn(II), Cd(II), and Hg(II) optical detection, *Inorg. Chem.* 53 (2014) 6149–6158.
- [28] P. Ravichandiran, S.A. Subramanian, S.-Y. Kim, J.-S. Kim, B.-H. Park, K.S. Shim, D.J. Yoo, Synthesis and anticancer evaluation of 1,4-naphthoquinone derivatives containing a phenylaminosulfanyl moiety, *ChemMedChem* 14 (2019) 532–544.
- [29] P. Ravichandiran, V.K. Kaliannagounder, A.P. Bella, A. Boguszewska-Czubara, M. Maslyk, C.S. Kim, C.H. Park, P.M. Johnson, B.-H. Park, M.-K. Han, A.R. Kim, D. J. Yoo, Simple colorimetric and fluorescence chemosensing probe for selective detection of Sn²⁺ ions in an aqueous solution: Evaluation of the novel sensing mechanism and its bioimaging applications, *Anal. Chem.* 93 (2021) 801–811.
- [30] P. Ravichandiran, S.A. Subramanian, A.P. Bella, P.M. Johnson, A.R. Kim, K.S. Shim, D.J. Yoo, Simple fluorescence turn-on chemosensor for selective detection of Ba²⁺ ion and its live cell imaging, *Anal. Chem.* 91 (2019) 10095–10101.
- [31] P. Ravichandiran, D.S. Prabhakaran, A.P. Bella, A. Boguszewska-Czubara, M. Maslyk, K. Dineshkumar, P.M. Johnson, B.-H. Park, M.-K. Han, H.G. Kim, D.J. Yoo, Naphthoquinone-dopamine linked colorimetric and fluorescence chemosensor for selective detection of Sn²⁺ ion in aqueous medium and its bio-imaging applications, *ACS Sustain. Chem. Eng.* 8 (2020) 10947–10958.
- [32] P. Ravichandiran, A. Boguszewska-Czubara, M. Maslyk, A.P. Bella, S.A. Subramanian, P.M. Johnson, K.S. Shim, H.G. Kim, D.J. Yoo, Naphthoquinone-based colorimetric and fluorometric dual-channel chemosensor for the detection of Fe²⁺ ion and its application in bio-imaging of live cells and zebrafish, *ACS Sustain. Chem. Eng.* 7 (2019) 17210–17219.
- [33] X. Feng, G.E. Fryxell, L.Q. Wang, A.Y. Kim, J. Liu, K.M. Kemner, Functionalized monolayers on ordered mesoporous supports, *Science* 276 (1997) 923.
- [34] H. Yang, Z.-G. Zhou, J. Xu, F.-Y. Li, T. Yi, C.-H. Huang, A highly selective ratiometric chemosensor for Hg²⁺ based on the anthraquinone derivative with urea groups, *Tetrahedron* 63 (2007) 6732–6736.
- [35] D. Phapale, A. Kushwaha, D. Das, A simple benzimidazole styryl-based colorimetric chemosensor for dual sensing application, *Spectrochim. Acta, Part A* 214 (2019) 111–118.
- [36] J. Sun, Y. Li, S. Shen, Q. Yan, G. Xia, H. Wang, A squaraine-based fluorescence turn on chemosensor with ICT character for highly selective and sensitive detection of Al³⁺ in aqueous media and its application in living cell imaging, *Spectrochim. Acta, Part A* 228 (2020) 117590.
- [37] Y. Li, Z. Li, T. Ablekim, T. Ren, W.-J. Dong, Rational design of tetraphenylethylene-based luminescent down-shifting molecules: photophysical studies and photovoltaic applications in a CdTe solar cell from small to large units, *Phys. Chem. Chem. Phys.* 16 (2014) 26193–26202.
- [38] R.G. Pearson, Hard and soft acids and bases, *J. Am. Chem. Soc.* 85 (1963) 3533–3539.
- [39] G. Singh, A. Singh Diksha, G. Sharma Sanchita, Pawan Shilpy, C. Espinosa-Ruiz, M.A. Esteban, Designing the recognition of Sn²⁺ ions and antioxidants: N-heterocyclic organosilatrane and their magnetic nanocomposites, *New J. Chem.* 44 (2020) 6238–6250.
- [40] X. Jiao, C. Liu, S. He, L. Zhao, X. Zeng, Highly selective and sensitive ratiometric near-infrared fluorescent probe for real-time detection of Hg²⁺ and its bioapplications in live cells, *Dyes Pigm.* 160 (2019) 86–92.
- [41] J. Du, J. Fan, X. Peng, H. Li, J. Wang, S. Sun, Highly selective and anions controlled fluorescent sensor for Hg²⁺ in aqueous environment, *J. Fluoresc.* 18 (2008) 919–924.
- [42] A.W. Czarnik, Supramolecular chemistry, fluorescence, and sensing, in: *Fluorescent chemosensors for ion and molecule recognition*, American Chemical Society, 1993, pp. 1–9.
- [43] P. Su, Z. Zhu, J. Wang, B. Cheng, W. Wu, K. Iqbal, Y. Tang, A biomolecule-based fluorescence chemosensor for sequential detection of Ag⁺ and H₂S in 100% aqueous solution and living cells, *Sens. Actuators, B* 273 (2018) 93–100.
- [44] J.M.V. Ngororabanga, Z.R. Tshentu, N. Mama, A highly selective and sensitive ESIPt-based coumarin-triazole polymer for the ratiometric detection of Hg²⁺, *New J. Chem.* 43 (2019) 12168–12177.
- [45] L. Bai, Y. Xu, L. Li, F. Tao, S. Wang, L. Wang, G. Li, An efficient water-soluble fluorescent chemosensor based on furan Schiff base functionalized PEG for the

- sensitive detection of Al^{3+} in pure aqueous solution, *New J. Chem.* 44 (2020) 11148–11154.
- [46] M. Kamaci, İ. Kaya, A highly selective, sensitive and stable fluorescent chemosensor based on Schiff base and poly(azomethine-urethane) for Fe^{3+} ions, *J. Ind. Eng. Chem.* 46 (2017) 234–243.
- [47] Z. Mermer, O. Yavuz, S.K. Atasen, Y. Alcay, I. Yilmaz, Architecture of multi-channel and easy-to-make sensors for selective and sensitive Hg^{2+} ion recognition through Hg-C and Hg-N bonds of naphthoquinone-aniline/pyrene union, *J. Hazard. Mater.* 124597 (2020).
- [48] P. Ravichandiran, S. Sheet, D. Premnath, A.R. Kim, D.J. Yoo, 1,4-Naphthoquinone analogues: Potent antibacterial agents and mode of action evaluation, *Molecules* 24 (2019) 1437.
- [49] W.S. Matthews, J.E. Bares, J.E. Bartmess, F.G. Bordwell, F.J. Cornforth, G.E. Drucker, Z. Margolin, R.J. McCallum, G.J. McCollum, N.R. Vanier, Equilibrium acidities of carbon acids. VI. Establishment of an absolute scale of acidities in dimethyl sulfoxide solution, *J. Am. Chem. Soc.* 97 (1975) 7006–7014.
- [50] M.J. Frisch, G.W. Trucks, H.B. Schlegel, G.E. Scuseria, M.A. Robb, J.R. Cheeseman, G. Scalmani, V. Barone, G.A. Petersson, H. Nakatsuji, X. Li, M. Caricato, A.V. Marenich, J. Bloino, B.G. Janesko, R. Gomperts, B. Mennucci, H.P. Hratchian, J.V. Ortiz, A.F. Izmaylov, J.L. Sonnenberg, Williams, F. Ding, F. Lipparini, F. Egidi, J. Goings, B. Peng, A. Petrone, T. Henderson, D. Ranasinghe, V.G. Zakrzewski, J. Gao, N. Rega, G. Zheng, W. Liang, M. Hada, M. Ehara, K. Toyota, R. Fukuda, J. Hasegawa, M. Ishida, T. Nakajima, Y. Honda, O. Kitao, H. Nakai, T. Vreven, K. Throssell, J.A. Montgomery Jr., J.E. Peralta, F. Ogliaro, M.J. Bearpark, J.J. Heyd, E. N. Brothers, K.N. Kudin, V.N. Staroverov, T.A. Keith, R. Kobayashi, J. Normand, K. Raghavachari, A.P. Rendell, J.C. Burant, S.S. Iyengar, J. Tomasi, M. Cossi, J.M. Millam, M. Klene, C. Adamo, R. Cammi, J.W. Ochterski, R.L. Martin, K. Morokuma, O. Farkas, J.B. Foresman, D.J. Fox, *Gaussian 09*, in, Wallingford, CT, 2009.
- [51] Y. Yang, X.-L. Ni, T. Sun, H. Cong, G. Wei, A highly selective and sensitive fluorescent chemosensor for Hg^{2+} based on a pyridine-appended π -conjugated ligand, *RSC Adv.* 4 (2014) 47000–47004.
- [52] S.-K. Ko, X. Chen, J. Yoon, I. Shin, Zebrafish as a good vertebrate model for molecular imaging using fluorescent probes, *Chem. Soc. Rev.* 40 (2011) 2120–2130.